Magnetic Anomaly Guidance System for Mine Countermeasures Using Autonomous Underwater Vehicles

Roy Wiegert
Naval Surface Warfare Center, Dahlgren Division, Coastal Systems Station
6703 W Highway 98, Panama City, FL 32407
wiegertrf@ncsc.navy.mil

***Abstract*- This paper describes a magnetic anomaly guidance system that, with support from the Office of Naval Research, is being developed for fully autonomous detection, localization and classification of ferrous mines in Very Shallow Water/Surf Zone (VSW/SZ) environments.**

The magnetic guidance system's hardware configurations and magnetic target signature processing methods specifically have been developed for autonomous guidance of small, maneuverable sensing platforms, such as Underwater Bottom Vehicles, (UBVs), to magnetic targets. The prototype magnetic anomaly guidance is a three-axis magnetometer-gradiometer comprised by an array of triaxial fluxgate magnetometers and triaxial accelerometers. This design allows development of magnetic gradient tensor contraction scalars that provide the basis for a unique method for magnetic guidance of UBVs to underwater and buried mines. The triaxial accelerometer array can be used for mitigation of the target-detection-range-reducing effects of large changes in sensor platform orientation.

Field test results indicate that a simple magnetic guidance algorithm based on comparison of the magnitudes of contractions of gradient tensor subsets measured by "primary guidance axes" of the sensor array will provide a robust and practical method for fully autonomous guidance of high- mobility UBVs to magnetic targets. Target detection range can be enhanced by using rotationally invariant tensor contractions for robust proximity sensing and "pseudo-robust" scalar total field quantities for "homing in on" magnetic targets. Sensor system stability and DLC performance also would be improved by the use of better, temperature-compensated magnetometers.

The results indicate that the magnetic anomaly guidance system and its method for target localization are particularly appropriate for homing in on magnetic targets from high-mobility sensing platforms such as small UBVs or Navy Divers.

I. INTRODUCTION

With support from the Office of Naval Research (ONR), NAVSEA-Coastal Systems Station (CSS) has participated in the development of magnetic sensing technologies that potentially will enhance the effectiveness of autonomous underwater vehicles (AUVs) for mine countermeasures (MCM) in littoral Very Shallow Water/Surf Zone (VSW/SZ) environments. In particular, CSS has developed an innovative magnetic anomaly sensing approach for detection, localization and classification (DLC) of magnetic targets such as underwater and buried mines [1,2,3]. The approach processes target magnetic anomaly signatures and develops magnetic scalar quantities that form the basis of a unique magnetic "Scalar Triangulation and Ranging (STAR)"[2] method for DLC of mines using high mobility sensing platforms such as AUVs or Navy divers. In particular the magnetic STAR method can be adapted for guidance of autonomous underwater bottom vehicles (UBVs) to underwater mines in challenging VSW/SZ environments.

This paper presents field test data from a prototype magnetic anomaly guidance system for UBVs. The data indicate that magnetic sensor designs based on the Scalar Triangulation and Ranging concept also would provide very effective mine DLC systems for other high-mobility sensing "platforms" such as Navy Explosive Ordnance Disposal (EOD) Divers.

Generally speaking, the physical basis for the use of magnetic anomaly sensors for DLC of underwater and buried mines is the magnetic fields $\mathbf{B}_A$ that emanate from magnetically polarized mines. The $\mathbf{B}_A$ fields constitute dc magnetic anomalies within the Earth's background field. The magnetic anomaly fields or "target signatures" contain implicit information that relates to the location and magnetic strength of the mines. The target signatures essentially are not affected by water turbulence, turbidity, bubble clouds, multi-path propagation effects or even intervening layers of mud or sand (for buried mines) that can limit the performance of other sensing technologies in VSW/SZ environments.

However, there are several challenges to practical use of magnetic sensors for DLC of mines from small, high-mobility sensing platforms such as UBVs or Navy EOD Divers:

- UBV operation in turbulent VSW/SZ environments typically will result in large changes in sensor platform orientation that can result in reduction of DLC range due to non-target-related changes in vector magnetic field measurements. Mobile sensor applications generally either require devices that measure magnetic field gradients, i.e., "gradiometers" or devices such as scalar magnetometers that are relatively insensitive to platform orientation. However, conventional gradiometry usually requires fairly uniform platform motion and scalar magnetometry does provide an efficient target DLC modality for UBVs.

0-933957-31-9 2002

Report Documentation Page

Form Approved
OMB No. 0704-0188

1. REPORT DATE	2. REPORT TYPE	3. DATES COVERED
01 SEP 2003	**N/A**	**-**

4. TITLE AND SUBTITLE	5a. CONTRACT NUMBER
Magnetic Anomaly Guidance System for Mine Countermeasures Using Autonomous Underwater Vehicles	5b. GRANT NUMBER
	5c. PROGRAM ELEMENT NUMBER
6. AUTHOR(S)	5d. PROJECT NUMBER
	5e. TASK NUMBER
	5f. WORK UNIT NUMBER
7. PERFORMING ORGANIZATION NAME(S) AND ADDRESS(ES) **Naval Surface Warfare Center, Dahlgren Division, Coastal Systems Station 6703 W Highway 98, Panama City, FL 32407**	8. PERFORMING ORGANIZATION REPORT NUMBER
9. SPONSORING/MONITORING AGENCY NAME(S) AND ADDRESS(ES)	10. SPONSOR/MONITOR'S ACRONYM(S)
	11. SPONSOR/MONITOR'S REPORT NUMBER(S)

12. DISTRIBUTION/AVAILABILITY STATEMENT
Approved for public release, distribution unlimited

13. SUPPLEMENTARY NOTES
See also ADM002146. Oceans 2003 MTS/IEEE Conference, Held in San Diego, California on September 22-26, 2003. U.S. Government or Federal Purpose Rights License, The original document contains color images.

14. ABSTRACT

15. SUBJECT TERMS

16. SECURITY CLASSIFICATION OF:			17. LIMITATION OF ABSTRACT	18. NUMBER OF PAGES	19a. NAME OF RESPONSIBLE PERSON
a. REPORT	b. ABSTRACT	c. THIS PAGE			
unclassified	**unclassified**	**unclassified**	**UU**	**9**	

- The small physical size, power and computational budgets of UBVs largely precludes the use of more conventional tensor gradiometry and scalar magnetometry approaches for target localization and magnetic anomaly guidance.
- The UBV's self magnetic signature due to electric drive motors and other electrical subsystems, will, unless mitigated, tend to overwhelm the very small target signatures, $\mathbf{B_A}$ and seriously degrade the practical DLC capabilities of any UBV-mounted magnetic sensor system. Consequently, the UBV signature should be reduced as much as possible and residual signature effects should reduced by judicious application of adaptive signature compensation techniques.

The Scalar Triangulation and Ranging- STAR concept for DLC of magnetic targets was specifically designed to meet the challenges presented by small, high-mobility UBV-type sensing platforms. Initial results from a prototype sensor demonstrated the validity of the STAR method for three-dimensional DLC of magnetic targets [3]. This paper presents additional test results that more explicitly demonstrate that the gradient-contraction-based STAR concept is particularly appropriate for adaptation into a relatively simple sensor system for fully autonomous guidance of UBVs to magnetic targets.

On continuation, this paper will present the following:

1. A brief technical background of magnetic anomaly sensing theory and techniques.
2. Technical details of the magnetic anomaly guidance system and its Scalar Triangulation method..
3. Results and discussion of field tests of the sensor system and its magnetic guidance parameters.

II. TECHNICAL BACKGROUND

In general, detection, localization and classification (DLC) of magnetic object relates to:

- The existence of vector magnetic fields $\mathbf{B_A}$ that emanate from the objects' net magnetization **M**. The $\mathbf{B_A}$ fields constitute "magnetic anomalies" within the Earth's background field.
- The relatively large and locally nearly constant magnetic field of Earth, $\mathbf{B_E}$. Since the relatively small target anomaly field is convolved with B_E , the Earth's field also complicates the process of DLC of magnetic objects using mobile sensing platforms.

At distances, *r*, greater than about three times a magnetic object's longest dimension, the "far-field" $\mathbf{B_A}$ of a magnetically polarized object is given by the well-known magnetostatic dipole equation.

$$\mathbf{B_A}(\boldsymbol{r},\mathbf{M}) = (\mu/4\pi)[\, 3(\mathbf{M}\bullet\boldsymbol{r})\boldsymbol{r}/r^5 - \mathbf{M}/r^3] \qquad (2.1)$$

In SI units, $\mathbf{B_A}$ (**r**) [Tesla, T] is the vector magnetic induction at a point defined by a position vector ***r*** [meters, m] relative to a vector magnetic dipole source **M** with units of Amperes x meter squared, Am^2. The parameter μ [Tm/A] is the magnetic permeability which for non-magnetic media, is approximately $4\pi \times 10^{-7}$ Tm/A, and $\pi = 3.14159...$

Direct measurements of $\mathbf{B_A}$ are complicated by the presence of the relatively very large Earth field $\mathbf{B_E}$. $\mathbf{B_E}$ has a nearly constant magnitude B_E of about ($\approx$) 50,000 nT (1 nT = 10^{-9} T) at the Earth's surface. However, (2.1) indicates that dipole fields decrease with the inverse cube of distance to the objects, i.e., $B_A \propto r^{-3}$. In particular, the B_A fields of mine-like targets drop off to nT and sub-nT levels at distances of a few meters from the targets. Therefore, $B_A << B_E$ except for field points that are measured very close to the target. Also, direct measurements of magnetic field actually involve measurement of a total field $\mathbf{B_T}$ that is the vector sum of $\mathbf{B_A}$ and $\mathbf{B_E}$, i.e., $\mathbf{B_T} = \mathbf{B_E} + \mathbf{B_A}$. The magnitude of B_T in Cartesian (XYZ) coordinates is

$$B_T = (B_{TX}^{\,2} + B_{TY}^{\,2} + B_{TZ}^{\,2})^{0.5} \qquad (2.2)$$

B_T is a rotationally invariant scalar that is not affected by changes in mobile sensor platform orientation. Unfortunately however, B_T doesn't provide a robust basis for target localization since in some regions of target space B_T may decrease as the target is approached. This non-robust behavior arises because locally the $\mathbf{B_A}$ field lines curve 360° through space while $\mathbf{B_E}$ is essentially constant in direction. Consequently, in some regions, components of the $\mathbf{B_A}$ fields point in the same direction as $\mathbf{B_E}$ and increase the magnitude of $\mathbf{B_T}$, in other regions the $\mathbf{B_E}$ and $\mathbf{B_A}$ fields point in opposite directions thereby decreasing the magnitude of $\mathbf{B_T}$.

While B_T by itself is non-robust, the Scalar Triangulation and Ranging method does develop a B_T -based "pseudo-robust" [2] quantity that can be used for longer range magnetic anomaly detection and guidance than the robust gradient (**G**)–based guidance parameters that are described in the following paragraphs..

The magnetic gradient tensor and magnetic gradiometry.

The gradient of $\mathbf{B_E}$ is quite small, typically $\nabla\, \mathbf{B_E} \approx 0.02$ nT/meter. Therefore, the effects of $\mathbf{B_E}$ can be greatly reduced by using sensors that measure the gradient of $\mathbf{B_T}$ (i.e., "gradiometers") since $\nabla\, \mathbf{B_T} \approx \nabla\, \mathbf{B_A}$. In magnetic gradiometry the measurements of gradient components of $\mathbf{B_A}$ provide the basis for target localization and classification.

The gradient, $\mathbf{G} = \nabla \mathbf{B_A}$, ($|\nabla \mathbf{B_A}(\mathbf{r})| \propto r^{-4}$) of the vector field of (2.1) is a second rank tensor whose matrix elements are given by the following expression [4].

$$(\nabla \mathbf{B})_{ij} \equiv G_{ij} \equiv \partial B_i/\partial r_j =$$

$$= -3(\mu/4\pi)[\mathbf{M}\bullet\boldsymbol{r}(5r_i r_j - r^2\delta_{ij}) - r^2(r_i M_j + r_j M_i)]\, r^{-7} \qquad (2.3a)$$

Eq. (2.3) constitutes a set of equations that relate measured gradient components with the unknown components of target position ***r*** and dipole moment **M**. In (2.3a), the r_i , M_i terms respectively refer to the X,Y,Z Cartesian components of ***r*** and **M**. ($r_1 \equiv X$, $r_2 \equiv Y$, $r_3 \equiv Z$ etc.). Magnetic gradiometry basically involves measurements of gradient components combined with rather complex methods for gradient tensor

"inversion" to determine components of *r* and M [4]. The complete gradient, G_T matrix is:

$$\mathbf{G} \equiv \begin{matrix} G_{xx} & G_{xy} & G_{xz} \\ G_{yx} & G_{yy} & G_{yz} \\ G_{zx} & G_{zy} & G_{zz} \end{matrix} = \begin{matrix} \partial B_x/\partial x & \partial B_x/\partial y & \partial B_x/\partial z \\ \partial B_y/\partial x & \partial B_y/\partial y & \partial B_y/\partial z \\ \partial B_z/\partial x & \partial B_z/\partial y & \partial B_z/\partial z \end{matrix}$$

$$\approx \begin{matrix} \Delta B_x/\Delta x & \Delta B_x/\Delta y & \Delta B_x/\Delta z \\ \Delta B_y/\Delta x & \Delta B_y/\Delta y & \Delta B_y/\Delta z \\ \Delta B_z/\Delta x & \Delta B_z/\Delta y & \Delta B_z/\Delta z \end{matrix} \qquad (2.3b)$$

The finite difference elements, $\Delta B_x/\Delta x$, $\Delta B_x/\Delta y$, $\Delta B_x/\Delta z$, etc, represent the fact that, in practice, the gradient components, $\partial B_x/\partial x$, $\partial B_x/\partial y$, $\partial B_x/\partial z$, etc.) are determined by measuring vector field components at spatially points along the XYZ axes, subtracting the field values at one point from the values at another and dividing the resultant differential field values by the separations ΔX, ΔY,ΔZ between the measuring points.

For conventional gradiometry the ΔX, ΔY,ΔZ are much smaller than the distance to target, *r*. However, the operational paradigm of mine DLC using UBVs requires the UBV to approach to within such close proximity to the mines that the approximations $G \propto r^{-4}$ and/or ΔX, ΔY,$\Delta Z << r$ may not be valid.

Some simplification of the gradient tensor measurement process can result from Maxwell's Equations for the divergence and curl of **B**, namely, $\nabla \bullet \mathbf{B} = 0$ and $\nabla \times \mathbf{B} = 0$. Then the sum of diagonal matrix elements is zero (i.e., $\partial B_x/\partial x+\partial B_y/\partial y + \partial B_z/\partial z =0$) and "across-diagonal" matrix elements are equal (that is $\partial B_x/\partial y = \partial B_y/\partial x$, $\partial B_x/\partial z = \partial B_z/\partial x$, and $\partial B_y/\partial z = \partial B_z/\partial y$) and measurement of five independent tensor components will completely determine the gradient tensor. The present work uses the aforementioned symmetry properties to construct the complete gradient tensor G_T and the corresponding total gradient contraction, C_T .

However, even with the reduced number of independent matrix components, the localization of magnetic targets through inversion of the gradient equations (2.3) typically requires operational constraints on sensor platform motion (e.g., a requirement for constant velocity) in addition to mathematical ambiguities and requirements that $G \propto r^{-4}$ and ΔX, ΔY,$\Delta Z >> r$, that may make the gradient tensor inversion approach more complex than is necessary for simple guidance of UBV-type sensing platforms or Navy Divers to magnetic targets.

A simplified approach to magnetic anomaly guidance can be based on the Scalar Triangulation and Ranging (STAR) method. The STAR method develops target localization information from sums-of-squares or "contractions" of the gradient tensor components [1-3]. In Cartesian coordinates, the mathematical operation of tensor contraction of (2.3) is given by the following expression:

$$C_T^2 = \sum_{i,j} (G_{ij})^2 = G_{xx}^2 + G_{xy}^2 + \ldots$$

$$\approx (\Delta B_X/\Delta X)^2 + (\Delta B_X/\Delta Y)^2 + \ldots \qquad (2.4)$$

The contraction, C_T of G_T, the full, nine component gradient tensor, , is a rotationally invariant and robust quantity. Here, rotational invariance implies that a quantity doesn't change as the sensor platform is rotated relative to the target. Consequently, by itself, a fully rotational invariant quantity such as C_T does not provide explicit directional control parameters that will immediately indicate when an UBV turns away from the target direction. However, as will be shown in the EXPERIMENTAL RESULTS section, partial, 3-component subsets of the magnetic anomaly gradient tensor can indeed provide a robust basis for guidance of UBVs or Navy Divers to magnetic targets.

III. TECHNICAL APPROACH

The need for a compact and practical magnetic anomaly guidance (or homing) system for small, high-mobility UBVs has led to a simplified adaptation of the STAR approach [2,3] for magnetic anomaly localization. The simplified guidance approach is based on the following:

(A) A magnetometer-gradiometer sensor system, shown in Figs. 1 and 2, that combines signals from a three axis, array of commercially available triaxial magnetometer/accelerometer (TMA) field sensing elements [3] . Each TMA contains a triaxial fluxgate, a triaxial accelerometer, A/D converter, microprocessor, and serial data RS232 interface. The magnetometers measure vector components of **B**-field at each point of the array. The accelerometers measure sensor platform orientation. Right and Left "Primary Guidance Axes", R and L in Fig. 2, are symmetrically disposed about a central symmetry axis S. For UBV guidance, magnetic signals from the primary guidance axes provide left-right directional control for "homing-in-on" magnetic targets.

(B) A processor uses the TMA data to develop magnetic gradient tensor and scalar total field quantities that implicitly contain target DLC information. In particular, partial three-component gradients (G_i) are calculated for each axis (i.e., each pair of TMAs). The partial gradients are used to construct the full gradient tensor, G_T. Primary magnetic anomaly guidance parameters C_R,C_L and C_T are developed through tensor contraction of the G_i and G_T gradient tensor matrix elements. "Pseudo-robust" sums of total fields (2.2) B_{TR}, B_{TL} and B_{TT} are also developed for the sensor axes to provide longer range detection and guidance.

Specific magnetic guidance parameters are developed in the following manner. Each TMA measures the X,Y,Z components of the local magnetic field $\mathbf{B_T}$. The B_{TX}, B_{TY}, and B_{TZ} data are processed to develop gradient and total field parameters. Gradient components are calculated for each sensor axis in the vehicle frame, namely $\Delta B_{Xi}/d_i$, $\Delta B_{Yi}/d_i$, and $\Delta B_{Zi}/d_i$ (where i denotes the respective R,L,B and S axes and d_i is the axis length). The gradient contraction C_i is calculated for each of the three axes using (2.4). For example, $C_R = [(\Delta B_{XR}/d_R)^2 + (\Delta B_{YR}/d_R)^2 + (\Delta B_{ZR}/\Delta d_R)^2]^{0.5}$ defines a partial gradient contraction of the three gradient components that are measured by TMAs 2 & 3.along the sensor system's

R-axis. The "total" gradient contraction C_T is given by the sum of squares of the full, nine component gradient tensor, G_T. Six components of G_T directly are obtained from direct field measurements and three components are obtained from the symmetry properties of G. Similarly, total field values B_{T1}, B_{T2} and B_{T3} are calculated for each of the three TMAs using (2.2). Then total field sums are calculated for each axis. The resulting pseudo-robust guidance parameters are $B_{TR} = B_{T2} + B_{T3}$, $B_{TL} = B_{T1} + B_{T2}$ and $B_{TT} = B_{T1} + B_{T2} + B_{T3}$.

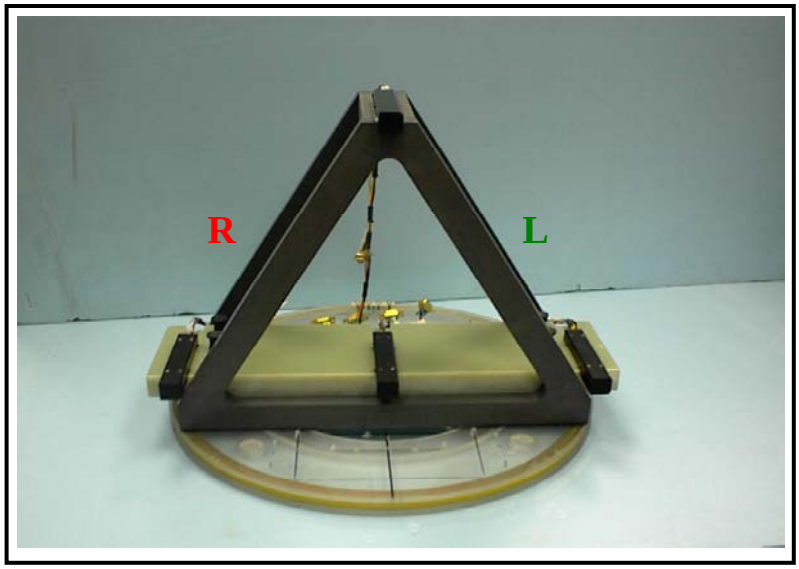

Fig. 1. Prototype gradiometer and magnetic guidance system. Triaxial Magnetometer-Accelerometers (TMAs) measure magnetic field and acceleration at each point of the array. The Right and Left (R and L) axes are the "Primary Guidance Axes" of the gradiometer.

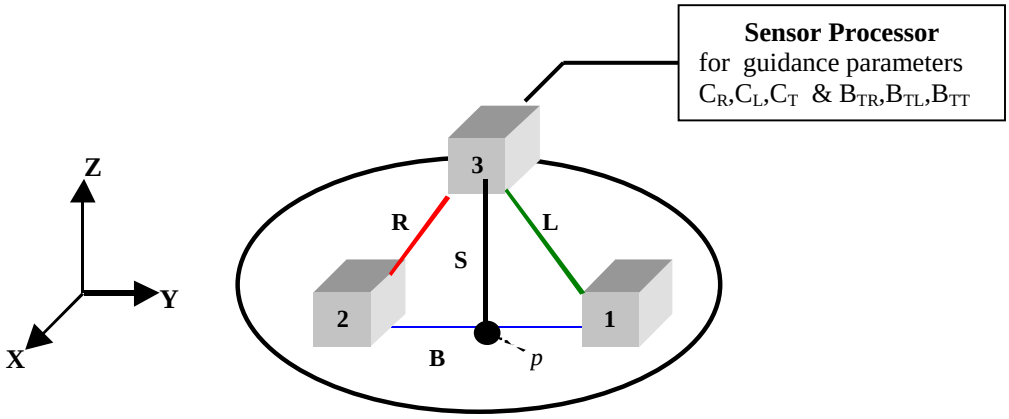

Fig. 2. Schematic of the geometrical configuration of the prototype magnetic anomaly guidance system. Three TMAs, 1,2,&3, are located at the vertices of an isosceles triangle. The plane of the triangle is perpendicular to the horizontal, XY plane of the circular sensor support platform. The Right (R) and Left (L) Primary Guidance Axes respectively are comprised TMAs 2&3 and TMAs 1&3. The R and L sides are each 33.8 cm long. A 27.0 cm symmetry axis (S) goes from TMA-3 to the midpoint (*p*) of Base Axis (B). TMAs 1 &2 comprise the 40.3 cm B-axis. The processor develops gradient contraction quantities that are used in the Scalar Triangulation and Ranging (STAR) method of magnetic target localization. For two dimensional localization of mines using this simple three axis array, the Primary Guidance Axis (R or L) that is closest to target develops the largest gradient contraction signal, C_R or C_L. Homing in on a target simply involves maneuvering the UBV under control of the Primary Guidance Axis signals to maintain $C_R = C_L$ and verifying increasing values of the Total gradient contraction, C_T, as the UBV approaches the target.

Extensive field tests were performed to verify that the magnetic STAR concept will provide a robust basis for fully autonomous guidance of UBVs to magnetic targets. The test range and procedures are indicated in Fig. 3. A magnetic dipole target was configured to approximate the anomaly field be developed by a 0.027 m^3 ferrous object in the Earth's magnetic field [5,6]. Data runs were performed with the target near the plane of the gradiometer support structure or 1 m below the base axis of the sensor. Consequently, the data represent the target signatures that an UBV would see for a mine located on or below the seafloor. Previous results [3] indicated that the sensor system was susceptible to "gradient drift". In order to quantify a putative temperature dependence for the sensor drift problem TMA temperature data were taken and processed simultaneously along with the magnetic anomaly data..

IV. RESULTS AND DISCUSSION

The data curves in Figs. 4-9 represent gradient contraction and total field sums from the Left and Right "Primary Guidance Axes" (i.e., C_L, C_R, B_{TL}, B_{TR},), total gradient contraction, (C_T) and the total field sum from all three TMAs (B_{TT}). Figures 4-6 show the variations in gradient contraction and total field values that were measured by the gradiometer/ guidance system as it was moved on tangential paths with headings of 135°, 180° and 270° and with closest point of approach (CPA) of 1.5 m as shown in Parts (b) and (c) of Fig. 3. For these, and other headings in Fig. 3(b), at the CPA the gradiometer's Left (L) axis was about 20 cm closer to the target than the Right (R) axis.

All magnetic-data curves are shown with the initial "offset" value at the beginning of the data run subtracted from subsequent data points.

The data in Figs. 4-6 show that within the gradiometer detection range of about 2 m, $C_T > C_L > C_R$. The quantity C_T should always be the largest of the three tensor contractions because it is the contraction of the full, nine component gradient tensor while C_L and C_R represent three-component subsets of the gradient tensor. Differences in gradient contraction amplitudes that are measured by the Left and Right Primary Guidance Axes reflect the influence of two factors that affect the value of the partial (sum of three components) gradient contraction that is measured by a given sensor axis. Namely, the magnitude of the partial gradient contraction C_i that is measured by a given axis (i) is a robust function of the axis's distance from the target and the length of the axis's projection in the target direction. Partial gradient contractions are not full rotational invariants; however, the sensor geometry shown in Figs. 1 and 2 exploits the symmetry properties of C_i to develop robust magnetic anomaly parameters that can be used to guide an UBV to magnetic targets. On the other hand, the tensor contraction, C_T, of the full, nine component gradient is a true rotational invariant that can provide an UBV with a more robust and longer range target-proximity-sensing capability.

In general, the scalar total field, B_T (2.2) is not a robust quantity; however, as indicated by the data of Figs. 4-6 and in [2], the absolute values of the displacements of B_{TL} and B_{TR}, the total field sums from, respectively, the Left and Right Axes actually may be used to provide a "pseudo-robust" modality for magnetic anomaly guidance. The data show that,

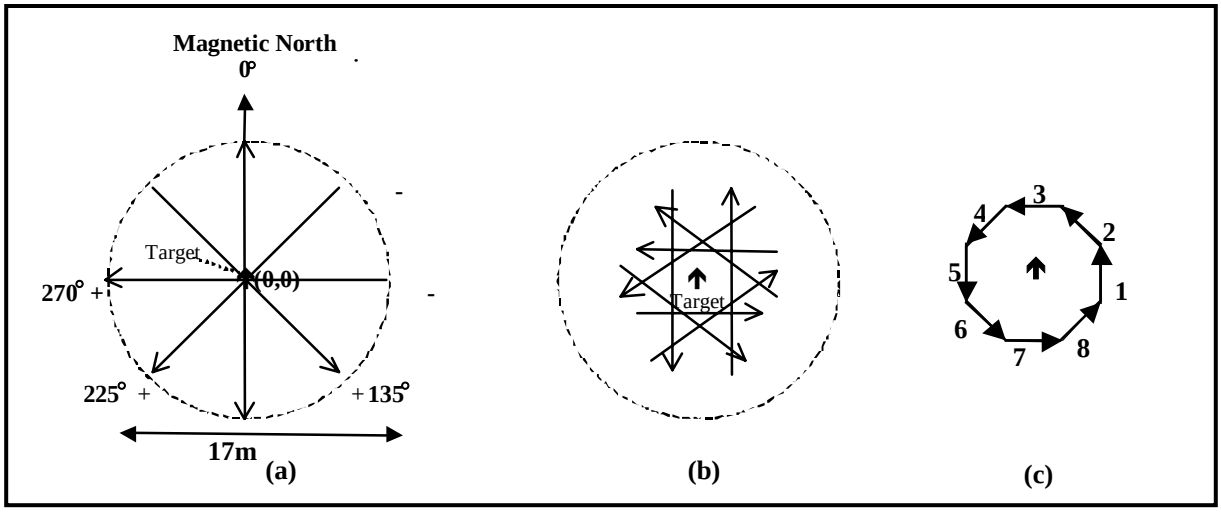

Fig. 3. Sketch of test range for gradiometer field tests. A permanent magnet dipole target with moment $|\mathbf{M}| = 14.5$ Am^2 and with declination of 0° and inclination 19° was fixed at the center (0,0) of the 17m diameter range. Data were taken by moving the sensor along the paths indicated by arrows in **(a) –(c)**. Part **(a)** represents "radial" approaches to target with the sensor path passing through the target position, while **(b)** shows "tangential" approaches to within 1.5 m from the target. Part **(c)** represents the two-dimensional closure of the tangential paths around target. For the eight tangential paths of **(b),(c)** the sensor system's Left Guidance Axis was closer to target than the Right Axis. Within the gradiometer detection range, the magnitude of Left-Axis gradient contraction C_L was larger than that of the Right Axis's C_R for all eight paths.

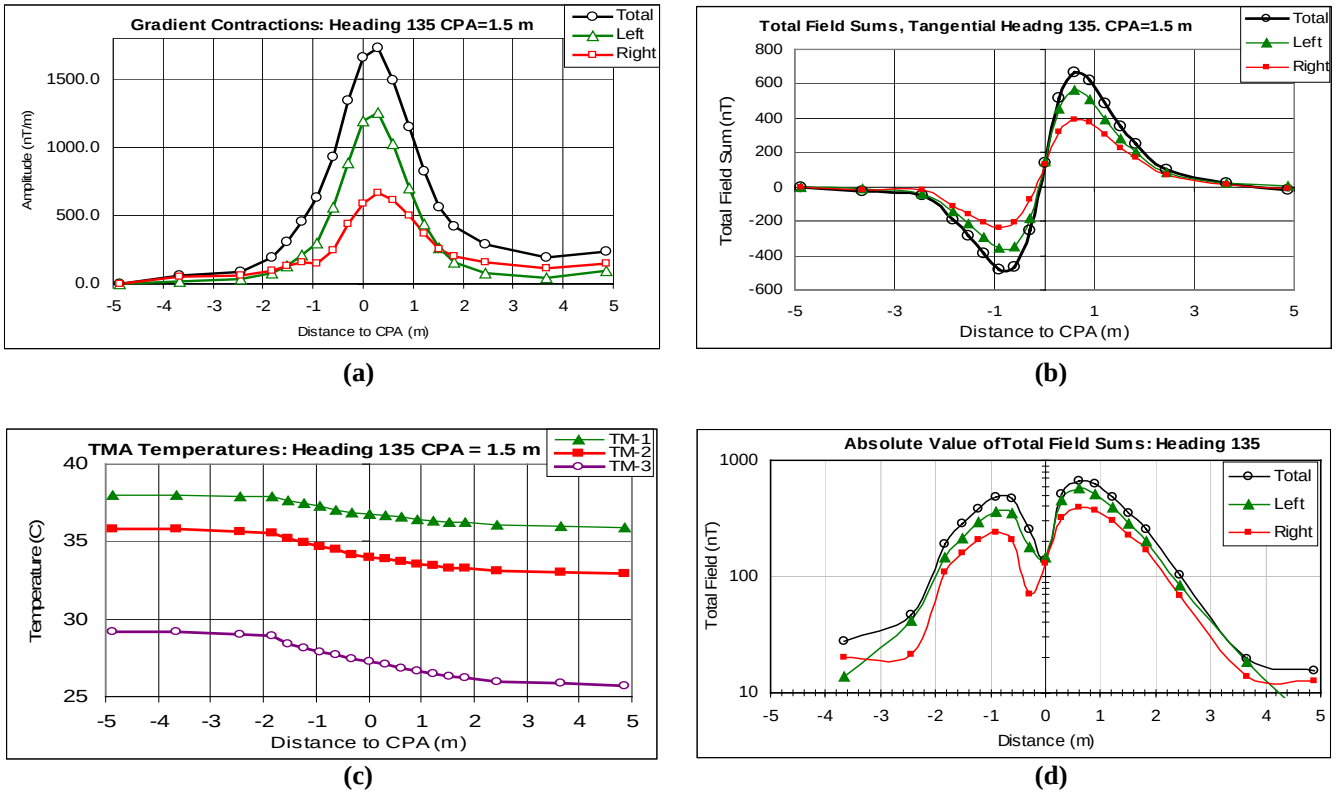

Fig. 4. Gradient contraction, total field and temperature data for the sensor system on a tangential approach to the target with a heading of 135° (path 6 of Fig. 3(c)). For these data curves, the left axis of the sensor system was closer to target than the right axis.

The Total, Left and Right curves of Part (a) respectively refer to the total gradient contraction, C_T, the partial gradient contraction for the left axis, C_L, and the partial gradient contraction for the right axis, C_R. Similarly, the Total, Left and Right curves of Parts (b) and (d) respectively refer to the sum of total fields measured by all three TMAs ($B_{TT} = B_{T1} + B_{T2} + B_{T3}$), the total field sum from the left axis TMAs ($B_{TL} = B_{T1} + B_{T3}$) and the total field sum from the right axis TMA ($B_{TR} = B_{T1} + B_{T2}$). Part (d) represents the total field data of Part(b) on a logarithmic scale. For this heading $B_{TL} > B_{TR}$ to a distance of 3.5-4 m.

Within the sensor detection range, the left axis gradient contraction, C_L, and total field sums B_{TL} are greater than the respective C_R and B_{TR} values for the right axis. For UBV guidance to a magnetic target, the condition $C_L > C_R$ provides a robust indication that the UBV should turn to the left in order to head directly toward the target. Likewise, the condition $B_{TL} > B_{TR}$ can provide a longer range albeit less robust indication that the target lies to the left of the UBV heading.

Variations in gradient contraction values at distances greater than 3 m are due to TMA sensor output drift. The sensor drift appears to correlate with the 2-3 °C changes in TMA temperature, that, as shown in Part (c) occurred during the data acquisition process.

with the Left Axis closer to target than the Right Axis, $|B_{TL}| > |B_{TR}|$ at target distances of up to 4 m. Thus, for some angles of approach to target, pseudo-robust total field sums can provide longer-range guidance and target detection than the robust gradient contraction data.

As indicated in Fig. 4 and explicitly shown in Fig. 7, sensor instabilities and target-detection-range-reducing output drift were found to correlate rather well with variations in TMA sensor temperature. Consequently, by solving the temperature-related sensor instability problem, the gradiometer's target detection range and magnetic anomaly guidance range can be enhanced. For example, as shown in Fig. 8, the effective magnetic target detection and guidance ranges were effectively doubled when the sensor system temperatures were kept relatively constant (± 0.5 °C).

Fig. 9 shows gradient contraction data that were taken along "radial paths" such as those indicated in Fig. 3 (a). These data (and the data of Figs. 4,5,6 & 8) illustrate the robustness and simplicity of the gradient contraction approach for magnetic anomaly guidance. For the data sets shown in Fig 9 (a), the sensor was pointed to the left of the target direction so that the Right Axis closer to target than the Left Axis and, consequently, $C_R > C_L$. The condition $C_R > C_L$ indicates that the sensor must turn to the right in order to head toward the target. Fig. 9(b) presents data for the same radial paths as Fig. 9(a) but with the sensor

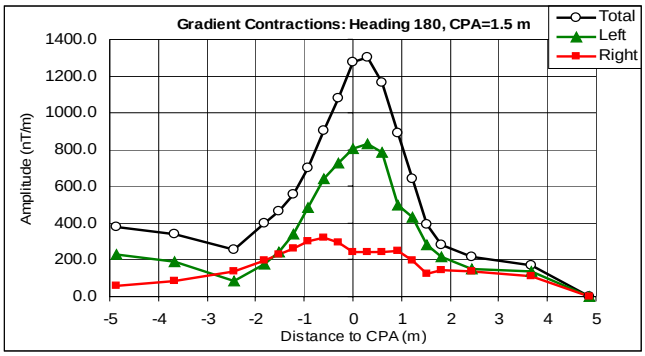

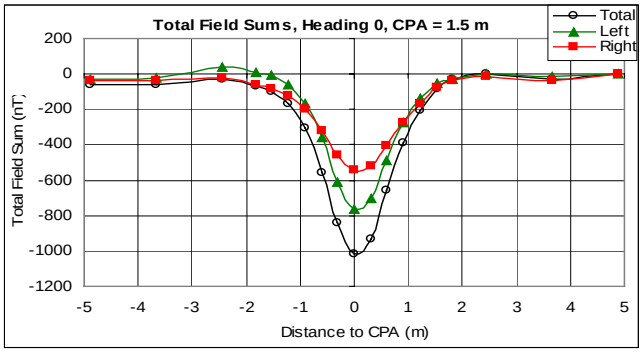

(a) **(b)**

Fig. 5. Gradient contraction and total field data for a tangential approach to the target on a heading of 180° (path 5 of Fig. 3(c)). The Left Axis of the sensor system was closer to target than the Right Axis and the magnitudes of the Left Axis gradient contraction and total field sums are greater than the respective values for the Right Axis. Sensor gradient instabilities were ≈ 200-400 nT/m. Variations in TMA temperatures were very similar to those of Fig.4(c).

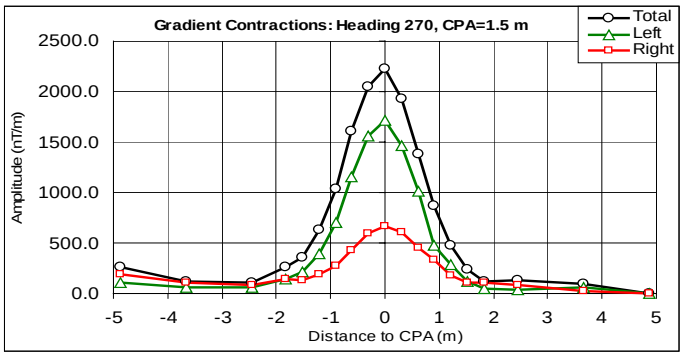

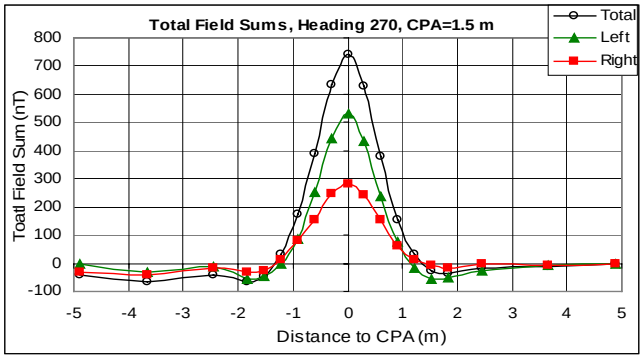

(a) **(b)**

Fig. 6. Gradient contraction and total field data for a tangential approach to the target on a heading of 270° (path 3 of Fig. 3(c). The Left axis of the sensor system was closer to target than the Right axis and the magnitudes of the Left axis gradient contraction and total field sums are greater than the respective values for the Right axis.

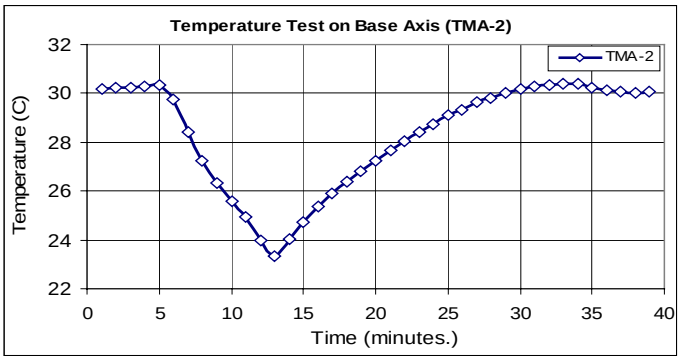

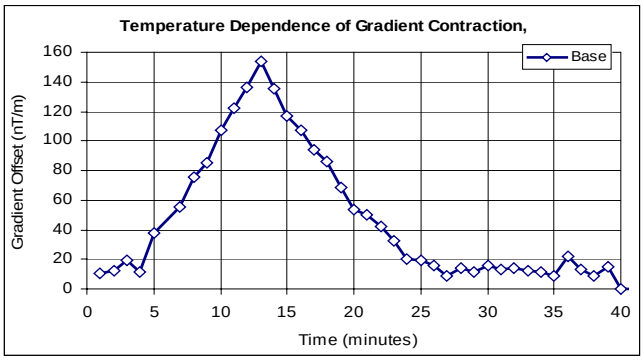

(a) **(b)**

Fig. 7. Correlation of TMA temperature and gradient contraction output drift. The gradiometer sensor was fixed on a heading of 0° with no target present and TMA-2 of the base axis was cooled for about 7 minutes. Part(a) shows the TMA temperature and Part (b) the corresponding variation in the Base axis gradient contraction, $C_{B.}$

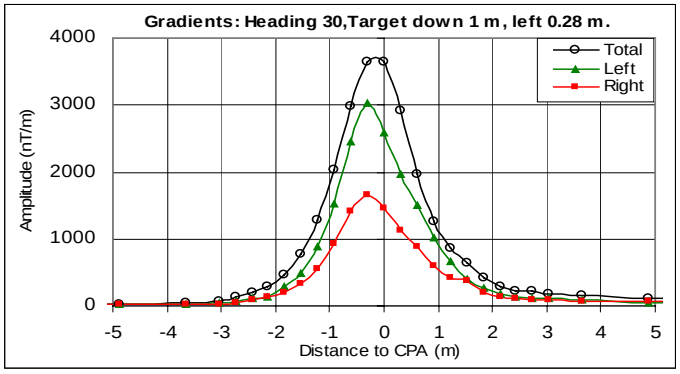

(a)

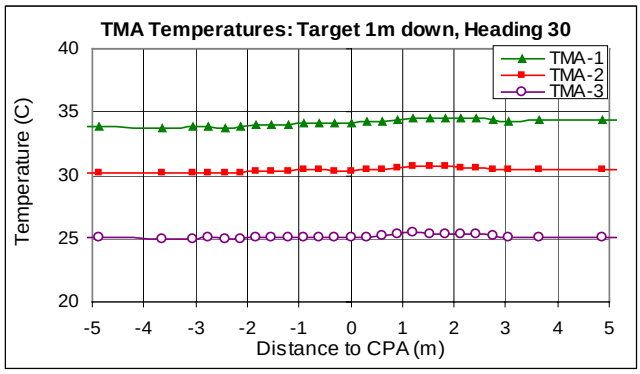

(b)

Fig. 8. Gradient contractions (a) and TMA temperatures (b) for the gradiometer on a tangential path toward the target located 1 m down and 0.28 m to the left of the sensor path. The experimental conditions were adjusted to minimize temperature changes. Consequently, there was relatively little drift in gradient contraction values and the detection range was enhanced to better than 3 m.

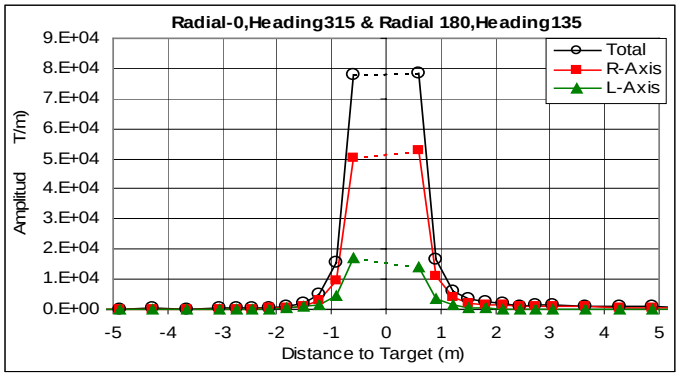

(a)

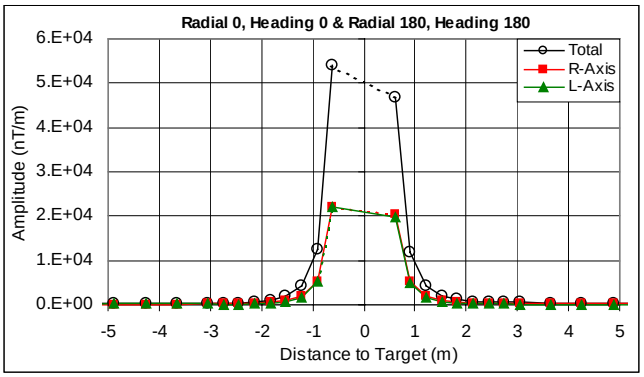

(b)

Fig. 9. Gradient contractions as the sensor system moved directly toward the target (to a CPA of 0.6 m) on radial paths of 0° and 180° (indicated by the vertical arrows in Fig. 3 (a)).

In Part (a) the sensor was rotated 45° to the left of the target bearing and so, at all points along the path, the Right Axis was closer to target than the Left Axis. Consequently, at all points along the radial paths of Part (a), the gradient contraction for the Right Guidance Axis, C_R, was greater than the gradient contraction for the Left guidance axis. C_L For guidance of an UBV to a magnetic target, the condition $C_R > C_L$ would constitute an error signal that indicates that the UBV must turn to the right in order to head directly toward the target. (Conversely, the condition $C_L > C_R$ would indicate that the UBV must turn to the left in order to head directly toward the target.)

In Part (b) the sensor platform has been rotated to point directly at the target so that the Left and Right guidance axes are equidistant from the target. Consequently the gradient contraction amplitudes from the two axes are essentially equal, that is $C_R = C_L$, at all points along the paths.

pointed directly at the target. In Fig. 9 (b) the condition of directly "homing in the target" is manifested by the following set of guidance parameter relations: $C_R = C_L$ and C_T, C_R and C_L all continually increase as the target is approached.

In summary, the data of Figs. 4-9 illustrate the following characteristics of the sensor system of Fig. 1 and its implementation of the Magnetic STAR approach to magnetic anomaly guidance for UBVs to bottom mines:

1. The gradient contraction signal developed by each Primary Guidance Axis (i.e., C_R and C_L) is a robust function of the distance from each axis to the target. Therefore, in order to head directly toward the target, the sensor platform/UBV should turn in the direction of the axis with the largest signal until the two guidance signal amplitudes are equal. As the UBV proceeds toward the target, all C_i–based guidance parameters should increase.

2. The total gradient contraction, C_T, of the full nine component tensor will provide longer-range detection and rotationally invariant proximity sensing for high mobility sensing platforms.
3. The sum of total fields from each Primary Guidance Axis (i.e., B_{TR} and B_{TL}) is a "pseudo-robust" function of the distance from each Axis to the target. The Axis closest to target usually will develop a larger absolute value of total field offset than the furthest Axis. This feature can be used to extend the target detection and guidance range beyond the gradient contraction's range [2].
4. Sensor system instabilities and signal level drift appear to strongly correlate with temperature changes in the triaxial magnetometer field sensing elements. Solution of the sensor instability problem would greatly enhance the effectiveness of the magnetic anomaly guidance approach.

The basic simplicity of the Magnetic STAR approach to magnetic anomaly guidance for UBVs is illustrated below in Fig. 10.

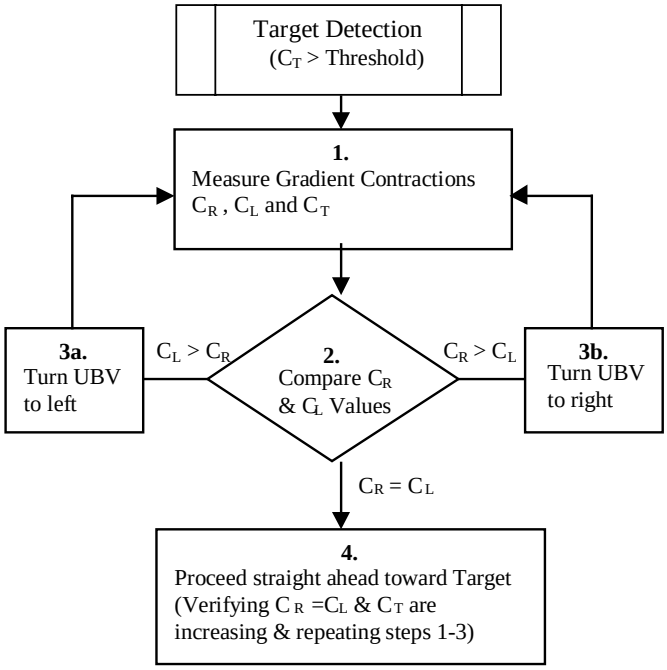

Fig. 10. Simplified flow diagram for an algorithm that would use signals from Primary Guidance Axes and the Magnetic STAR method for fully autonomous guidance of UBVs to magnetic targets.

V. CONCLUSION

The magnetic anomaly guidance system for UBVs that is described in this paper represents an adaptation of the more general, three-dimensional, Scalar Triangulation and Ranging (STAR) approach to detection, localization and classification of magnetic targets such as underwater and buried mines. Field test data and a consideration of the physical nature of magnetic anomaly fields indicate that a simple, three-axis gradiometer configuration will provide very effective, robust and practical gradient-contraction-based magnetic anomaly guidance for UBVs searching for mines on and buried under the sea bottom.

Furthermore, the power of the STAR approach for DLC of mines can be enhanced by increasing the number of field sensing elements of the array. For example, a five-primary-axis sensor system geometry can provide full, three-dimensional target detection, localization and classification capabilities. Such a design could be made sufficiently compact to provide a practical and effective mine DLC system for Navy Divers.

The relatively large size of the present sensor prototype is a consequence of the instabilities of the "TMA" field sensing devices. More stable field-sensing elements, in particular TMA devices that do not exhibit the temperature-dependent instabilities that are manifest in the field-test data would allow development of much more compact and effective magnetic anomaly guidance systems for high-mobility autonomous sensing platforms such as UBVs or Navy Divers.

ACKNOWLEDGEMENTS

This work was supported by the Office of Naval Research and performed for the Surf Zone Reconnaissance Project of ONR's Very Shallow Water Mine Countermeasures Program.

At the Coastal System Station, the following contributions are gratefully acknowledged: Brian Price developed the sensor system's data processing system and provided invaluable support for the initial phases of this work. Jalal Hyder helped collect and analyze field test data. Eric Tuovila helped enable construction of the sensor support structure.

REFERENCES

[1] R.F. Wiegert, and B.L. Price, "Magnetic sensor development for mine countermeasures using autonomous underwater vehicles", in Wood-Putnam, J. (Ed.), *Information Systems for Divers and Autonomous Vehicles Operating in Very Shallow Water and Surf Zone Regions*, Proceedings of SPIE, Vol. 4039, pp. 93-103, 2000.

[2] Wiegert, R.F. and Price, B.L., U.S. Patent 6,476,610 "Magnetic Anomaly Sensing System and Methods for Maneuverable Sensing Platforms."

[3] R.F. Wiegert, B.L. Price and J. Hyder, "Magnetic anomaly sensing system for mine countermeasures using high mobility autonomous sensing platforms", MTS/IEEE OCEANS 2002 Conference Proceedings, pp. 937-944.

[4] Wynn, W.M., Frahm, C.P., Carroll, P.J., Clark, H., and Wynn, M.J., "Advanced superconducting gradiometer/magnetometer arrays and a novel signal processing technique," IEEE Trans. Mag., **MAG-11**, pp. 701-707, (1975).

[5] Altschuler, T.W., "Shape and orientation effects on magnetic signature prediction for unexploded ordnance", UXO Forum 1996, (Williamsburg, VA, March 26-28, 1996), Conference Proceedings, pp.282-291.

[6] Lathrop, J.D., Shih, H., and Wynn, W.M., "Enhanced clutter rejection with two parameter magnetic classification for UXO", in Dubey, A.C., Harvey, J.F., Broach, J.T., and Dugan, R.E., (Eds), *Detection and Remediation Technologies for Mines and Minelike Targets IV*, Proceedings of SPIE, pp. 37-51, (1999).